THE ASTRONOMICAL JOURNAL

VOLUME 79 September 1974 ~ No. 1424 NUMBER 9

Optical identifications and radio spectra of sources found by the Michigan 8-GHz survey

G. W. Brandie*
Radio Astronomy Observatory, The University of Michigan, Ann Arbor, Michigan 48104

A. H. Bridle
Astronomy Group, Department of Physics, Queen's University at Kingston, Ontario, Canada
(Received 6 May 1974)

Optical counterparts have been found or confirmed for over 80% of the 55 sources found by an 8-GHz survey of $\simeq$0.8 steradian of sky between declinations $-4°$ and $+5°$. More than two-thirds of the identifications are with stellar objects. The 1.4- to 13.5-GHz spectra of the sources have been determined and classified using a radio analogue of the optical "two-color" diagram. The galaxies cluster in a region of the "two-color" diagram different from that occupied by the QSS. The sources have thus been divided into two main spectral classes —class "G", consisting entirely of nonvariable galaxies and empty fields, and class "Q", consisting of variable stellar objects with only a small proportion of "deviant" galaxies. Some of the stellar objects are neutral in color and may be quasars of very high redshift.

INTRODUCTION

THE discovery of a class of "centimetric excess" radio sources (Dent and Haddock 1965), some of which were soon found to be variable at microwave frequencies (Dent 1965) showed that the then-existing-metre- and decimetre-wavelength surveys did not provide fully representative samples of the extra-galactic radio source population. Recently, source samples have been selected at 1.4 GHz (Bridle, Davis, Fomalont, and Lequeux 1972a and references therein), at 2.7 GHz (Wall *et al.* 1971; Shimmins 1971; Shimmins and Bolton 1972) and at 5.0 GHz (Davis 1971; Pauliny-Toth *et al.* 1972; Pauliny-Toth and Kellermann 1972) to improve documentation of the microwave source population. These studies have found increasing fractions of sources with strong microwave emission at successively higher selection frequencies (e.g., Pauliny-Toth *et al.* 1970).

One of us (GWB) surveyed ~0.8 steradians of sky at 8.0 GHz (λ3.8 cm), the highest frequency to date at which an unbiased source survey has been carried out. This paper presents the list of sources found by that survey (Sec. II) and describes their optical identifications (Sec. III), radio spectra (Sec. IV), and variability (Sec. V), based on measurements made at six frequencies in the range 1.4–13.5 GHz.

I. OBSERVATIONS

A. The 8.0-GHz Survey

The 8.0-GHz finding survey and the subsequent 8.0-GHz observations were made with the 85-ft telescope of the University of Michigan Radio Astronomy Observatory. The dual-channel, Dicke-type radiometer employed tunnel-diode amplifiers with 1-GHz RF bandwidths and 700-K system temperatures. The antenna beamwidth was 5.9 arcmin. The effects of atmospheric noise fluctuations were minimized by switching the radiometer input between two off-axis feeds providing beams separated by 12.6 arcmin. Both feeds accepted linear polarization with the E-vector north–south.

The survey observations consisted of 24-h meridian transit scans across all right ascensions having $|b| > 15°$ at each of 91 equally-spaced declinations between $+5°$ and $-4°$ (epoch ~1969.0). During the survey, the reference feed was at the same declination as the main feed so that unresolved sources produced both a positive and a negative output response. The survey records were examined for source-like responses with amplitudes corresponding to peak flux densities greater than about

* Present address: Astronomy Group, Department of Physics, Queen's University at Kingston, Ontario, Canada.

0.6 Jy [1 Jy $=10^{-26}$ W m^{-2} Hz^{-1}] (approximately four times the rms noise), without reference to existing source catalogues. These "suspect" sources were validated by making repeated right ascension and declination scans across the survey positions. The sources found and confirmed by these procedures (described in more detail by Brandie 1972a) provide an unbiased, noise-limited sample of the intense radio source population at 8 GHz. The sample is expected to be 100% complete above 1.2 Jy, ~80% complete above 0.8 Jy, and ~60% complete above 0.6 Jy.

B. The 8-GHz Flux Densities

The sources were reobserved at 8 GHz to improve their measured positions and flux densities. Positions were measured relative to those of eleven unresolved sources determined to ~1 arcsec accuracy by Wade (1970), Wade *et al.* (1970), and Fomalont and Moffet (1971). The rms scatter in the position calibration was $1^s.7$ in right ascension and 23 arcsec in declination.

Flux densities were measured using procedures described by Dent and Haddock (1966) and Stull (1971). The flux-density scale was defined by adopting the 8-GHz flux densities listed in Table I, which have been revised from those of Dent and Haddock (1966) to conform with the spectrum of Cas A given by Kellermann *et al.* (1969).

Most of the sources were observed repeatedly between November 1967 and May 1972. These measurements have been analyzed for indications of variability (Brandie 1972b); the variability of the sources is discussed further in Section V of this paper.

C. The 1.4-GHz Observations

The observations at 1.4 GHz were made in August 1973 with the 300-ft meridian transit telescope at the National Radio Astronomy Observatory, Green Bank, West Virginia. (Operated by Associated Universities, Inc., under contract with the National Science Foundation.) Four independent feeds and radiometers mounted around the telescope focus were used as described by Bridle, Davis, Fomalont, and Lequeux (1972a; henceforth BDFL) to map an area of sky ~55 arcmin in right ascension by ~35 arcmin in declination centered on each 8-GHz source position. The data were reduced as described by BDFL, except that the effective antenna beamwidth for our observations was 9.85 arcmin in right ascension by 10.7 arcmin in declination, due to different smoothing of the data.

The flux-density scale was normalized to that of BDFL by adopting their 1.4-GHz flux densities (see Table I) for seven sources which are not resolved or confused at 1.4 GHz at the 300-ft telescope, and which are not known to vary at this frequency. The standard error of the normalization was 0.7%. Above $\delta=-5°$, the BDFL flux-density scale is identical to those of Kellermann *et al.* (1969), and the Parkes catalogue (Ekers 1969) at 1.4 GHz. It has also been shown (Fomalont, Bridle, and Davis, in preparation) to be consistent with the Westerbork 1.4-GHz scale (Katgert *et al.* 1973).

D. The 2.7-GHz Observations

The observations at 2.695 GHz were made in September 1972, January, and April 1973, also with the NRAO 300-ft transit telescope. A three-feed configuration was used with one feed on the electrical axis of the telescope; when this feed was pointed to the declination of a source, the transit was also observed at half-power to the north and to the south using the other feeds. Four independent load-switched radiometers with 140-K system temperatures and 100-MHz RF bandwidths recorded two senses of circular polarization at the on-axis feed, and one circular polarization at each of the off-axis feeds. This observing procedure allowed the apparent declination of a source to be determined at every transit, so that all flux densities could be corrected for the declination pointing of the telescope. Flux densities were derived from the information obtained from all three feeds. Transit times in the on-axis feed only were used to obtain right ascensions for each source.

The flux-density scale was normalized to that of Kellermann, Pauliny-Toth, and Tyler (1968) by adopting their 2.7-GHz flux densities (see Table I) for six sources which are not known to vary at this frequency. The standard error of the normalization was 0.8%. Comparison of our flux densities for these six sources with those of Wall *et al.* (1971) showed their 2.7-GHz scale to be 5.5±0.8% higher than ours.

The positional calibration of the telescope was determined with reference to positions of 23 sources in the declination range of the survey determined to ~1 arcsec accuracy at 2.7 GHz with the Malvern and NRAO interferometers (Wade 1970; Adgie *et al.* 1972; Brosche *et al.* 1973). The rms scatter in this calibration was $\sim 0^s.5$ in right ascension and ~12 arcsec in declination.

E. The 6.63-GHz Observations

The observations at 6.63 GHz were made on various occasions between February 1970 and October 1972 with the 150-ft telescope at the Algonquin Radio Observatory, Lake Traverse, Ontario. (Operated as a national radio astronomy facility by the National Research Council of Canada.) The receiver was a load-switched cooled parametric amplifier system with a 450-K system temperature and a 250-MHz RF bandwidth. The antenna beamwidth was close to 3.9 arcmin.

Observations were made by repeated scans in equatorial coordinates. Apparent positions determined by

TABLE I. Flux densities adopted for calibration at the NRAO 300-ft and Michigan 85-ft telescopes.

	Source	Flux density (Jy)
1.4 GHz		
	0034−01	4.30
	0035−02	6.25
	0240−00	4.87
	0305+03	7.24
	0500+01	2.21
	2128+04	3.98
	2210+01	2.60
2.7 GHz		
	0034−01	2.40
	0035−02	3.83
	0240−00	2.99
	0305+03	5.05
	2128+04	2.97
	2210+01	1.70
8.0 GHz		
	Cas A	629.6 (1964.4)
	3C 123	10.6
	3C 274	49.4
	3C 353	15.6
	3C 405	214.4

an on-line computer at the end of each scan were used to adjust the telescope pointing at the time of the observations. The final off-line reduction fitted the scans with a variable-width Gaussian response on a third-order polynomial baseline to deal with occasional fluctuations in atmospheric emission. The variation of telescope gain with orientation was determined by observing several intense sources over a wide range of zenith angles.

The flux-density scale was defined by adopting a value of 12.5 Jy for 3C 123. This flux density is consistent with the spectrum of 3C 123 between 1.4 and 10.6 GHz defined by the data of Kellermann *et al.* (1969), Wilson and Penzias (1966), Doherty *et al.* (1969), Dent (1972), and Kellermann and Pauliny-Toth (1973), and is identical to that adopted by Medd *et al.* (1972) at this frequency.

F. The 10.6-GHz Observations

The observations at 10.6 GHz were made between February 1970 and July 1972 with the 150-ft telescope at the Algonquin Radio Observatory. The receivers were a 10.63-GHz tunnel-diode system with an 1100-K system temperature and a 1250-MHz RF bandwidth, and later a 10.52-GHz cooled parametric amplifier system with a 120-K system temperature and 100-MHz RF bandwidth. The effective beamwidths of these systems were close to 2.8 and 2.7 arcmin, respectively.

The observing procedure was similar to that at 6.63 GHz, except that atmospheric effects were minimized by use of a beam-switching system in which the radiometer input was switched between a feed on the electrical axis of the telescope and another providing a beam 8.1 arcmin lower in elevation.

The flux-density scale was defined by adopting a flux density of 8.0 Jy (integrated), 7.9 Jy (peak) for 3C 123. This flux density is consistent with the spectrum of 3C 123 defined by the data listed in Sec. I-E, and is identical to the flux density adopted at this frequency by Medd *et al.* (1972).

G. The 13.5-GHz Observations

The observations at 13.5 GHz were made in October 1972 with the 150-ft telescope at the Algonquin Radio Observatory. The receiver was a 13.50-GHz parametric amplifier system with a 300-K system temperature and a 300-MHz RF bandwidth. The antenna beamwidth was close to 2.1 arcmin. The observing method was similar to that used at 10.63 GHz.

The flux-density scale was defined by adopting a peak flux density of 20.4 Jy for DR 21 (Dent 1972). The resulting peak flux density for 3C 123 of 6.2±0.2 Jy is consistent with extrapolation of the spectrum derived from the data described in Sec. I-E.

II. THE SOURCE LIST

Table II gives data on the 55 sources in the 8-GHz survey. Column (1) gives the source name, in Parkes-type notation. It is recommended that sources not previously cataloged be referred to by the source name from column (1) with the prefix MA, e.g., MA 0829+04. Columns (2) and (3) give the 1950.0 right ascension and declination for each source, with their standard errors. These positions were obtained by taking weighted averages of the positions from our own 2.7- and 8.0-GHz observations and those in the literature cited in Table III. If some measurements had estimated errors less than half the standard error in the overall weighted average, then only the more precise positions were included in the final weighted average. Thus, many of the listed positions are those measured with high-resolution interferometers, as will be evident from their assigned errors. The positions of sources denoted by an "A" in the "Notes" column were determined by E. B. Fomalont and ourselves (unpublished) using the NRAO three-element interferometer at 2.7 and 8.1 GHz. Column (4) of Table II gives the galactic latitude of the tabulated position to the nearest degree. Columns (5) to (10) list flux densities of the sources at 1.4, 2.7, 6.63, 8.0, 10.6, and 13.5 GHz, from our own observations supplemented by data from the references cited in Table III. For variable sources, the ranges of flux density observed to date are given in the appropriate columns. Where repeated observations have provided no evidence for variability, a weighted mean is given with its standard error. Column (11) gives the optical identifications of the sources, based on our inspection of the Palomar Sky Survey prints and plates at the positions given in Columns (2) and (3) (see Sec. III for details). Column (12) gives other common names

TABLE II. The source catalog.

(1)	(2)	(3)	(4)	(5)	(6)	(7)	(8)	(9)	(10)	(11)	(12)	(13)
				Flux densities								
Source name	Right ascension 1950.0	Declination 1950.0	b	1.4 GHz	2.7 GHz	6.6 GHz	8.0 GHz	10.6 GHz	13.5 GHz	ID	Other names	Note
0034−01	00 34 30.54±0.07	−01 25 40.2± 4.1	−64	4.20±0.15	2.42±0.08	···	1.30±0.04	0.92±0.04	···	GAL	3C15, PK, OB−057	···
0035−02	00 35 47.13±0.13	−02 24 07.7± 2.3	−64	6.27±0.22	3.87±0.09	···	2.20±0.10	1.82±0.08	1.57±0.13	GAL	3C17, PK, OB−061	···
0038−02	00 38 24.22±0.01	−02 02 58.6± 0.3	−64	0.88±0.05	0.53±0.05	···	0.96±0.08	···	1.00±0.20	QSS	PK0038−020	AB
0055−01	00 55 01.5 ±0.2	−01 39 46 ± 5	−64	5.34±0.19	3.14±0.13	1.90±0.05	1.69±0.06	1.44±0.11	···	GAL	3C29, PK, OB−092	B
0056−00	00 56 31.78±0.03	−00 09 18.4± 0.4	−63	2.16/2.44	1.92±0.04	1.20±0.06	1.23±0.04	···	0.88±0.21	QSS	4C−0.06, PK, OB−094	···
0106+01	01 06 04.50±0.02	+01 19 00.9± 0.4	−61	1.15/1.83	1.07/2.86	2.14/3.54	2.53/4.55	2.21/3.79	···	QSS	4C+1.02, PK, OC012	···
0111+02	01 11 08.54±0.01	+02 06 25.3± 0.2	−60	0.70±0.04	0.58±0.03	···	0.82±0.10	···	1.34±0.23	GAL	OC019, GC	A
0112−01	01 12 44.29±0.21	−01 42 56.5± 2.8	−64	1.01±0.05	1.05±0.04	···	1.00/1.55	1.15±0.1	1.13±0.15	BSO	OC−022, PK0112−017	···
0119+04	01 19 21.3 ±0.11	+04 06 46 ± 2	−58	1.42±0.06	1.83±0.04	···	2.12±0.06	···	1.92±0.16	BSO	OC033	···
0122−00	01 22 55.20±0.03	−00 21 30.7± 0.5	−62	1.48/1.77	1.00/1.44	1.15±0.10	1.50±0.13	1.05±0.15	2.38±0.15	QSS	4C−0.10, PK, OC−038	B
0123−01	01 23 27.0 ±0.8	−01 37 07 ±30	−63	6.75±0.23	3.21±0.15	···	(1.02)	···	···	GAL	3C40, PK, OC−039	C
0237−02	02 37 13.76±0.01	−02 47 34.5± 0.2	−54	0.31±0.04	0.38±0.03	···	0.77±0.03	···	0.67±0.11	BSO	OD−062, PK0237−027	A
0240−00	02 40 07.09±0.04	−00 13 30.7± 0.6	−52	4.98±0.17	2.85±0.11	1.68±0.05	1.45±0.06	1.00±0.03	1.11±0.20	GAL	3C71, PK, OD−067	···
0305+03	03 05 48.8 ±0.9	+03 55 14 ± 2	−45	7.16±0.25	4.89±0.12	2.90±0.30	2.55±0.05	2.37±0.15	2.11±0.29	GAL	3C78, PK, OE010	···
0336−01	03 36 59.0 ±0.23	−01 56 17 ± 2	−42	1.96/2.44	1.81/3.17	2.08/3.25	2.05/4.85	1.89/3.70	3.76±0.19	QSS	CTA26, PK, OE−063	B
0404+03	04 04 47.8 ±0.8	+03 32 53 ±10	−34	5.40±0.19	2.97±0.07	1.99±0.17	1.53±0.05	···	0.97±0.10	GAL?	3C105, PK, OF007	D
0420−01	04 20 43.53±0.02	−01 27 28.1± 0.7	−33	1.03/2.24	1.14/2.16	1.42/2.58	1.42/2.82	1.26/2.70	1.76±0.18	QSS	PK, OF−035, DA129	···
0422+00	04 22 12.44±0.02	+00 29 17.7± 0.4	−32	0.88/1.60	0.61/1.29	···	0.54/1.68	0.65/1.31	1.03±0.18	?	PK, OF038	AB
0440−00	04 40 05.29±0.03	−00 23 20.7± 0.5	−28	3.18±0.08	2.72/4.23	1.97/3.05	1.65/3.44	1.27/2.76	1.10±0.20	BSO	NRAO190, PK, OF−067	···
0500+01	05 00 45.35±0.15	+01 58 50 ±13	−23	2.18±0.08	2.31±0.04	1.68±0.05	1.41±0.04	1.36±0.08	0.94±0.10	□	OG003	···
0723−00	07 23 17.86±0.05	−00 48 54.6± 0.7	+07	2.25/3.10	1.85/3.01	1.97/2.50	1.66/2.71	1.53/2.21	1.73±0.28	NSO	DW, OI−039	···
0736+01	07 36 42.53±0.03	+01 44 00.3± 0.3	+11	2.34/2.89	2.02/2.42	1.52/2.42	1.51/2.39	1.26/2.40	0.86±0.21	QSS	PK, OI061	···
0743−00	07 43 21.05±0.02	−00 36 55.2± 0.3	+12	0.79±0.04	1.35±0.06	1.86/2.08	1.39/2.42	1.36/2.05	1.11±0.19	NSO	OI−072, PKO743−006	B
0829+04	08 29 10.87±0.02	+04 39 50.9± 0.4	+24	0.58±0.04	0.59±0.04	···	0.45/0.97	0.68±0.13	0.84±0.12	NSO	···	AB
0906+01	09 06 35.19±0.02	+01 33 48.1± 0.5	+31	1.22±0.04	0.86±0.05	0.82±0.10	0.71/1.42	0.97/1.61	1.26±0.18	QSS	4C+1.24, PK, OK011	···
0922+00	09 22 33.7 ±1.1	+00 32 13 ±14	+34	0.92±0.13	0.70±0.04	0.70±0.10	0.51/1.35	0.65±0.15	0.66±0.18	QSS	OK037, PK0922+005	···
1055+01	10 55 55.37±0.02	+01 50 03.0± 0.3	+53	3.10±0.08	2.94±0.08	2.86/3.50	2.62/4.44	2.66/3.63	3.10±0.44	BSO	4C+1.28, PK, OL093	···
1148−00	11 48 10.15±0.08	−00 07 12.9± 0.4	+59	3.09±0.11	2.43±0.09	1.63±0.03	1.60±0.03	1.14±0.11	1.16±0.12	QSS	4C−0.47, PK, OM−080	B
1219+04	12 19 49.3 ±0.4	+04 30 03 ±11	+66	0.78±0.04	0.76±0.03	1.12±0.35	0.79/1.76	0.81/1.57	0.63±0.20	BSO	PK, DA321	B
1226+02	12 26 33.24±0.2	+02 19 42.6± 1.1	+64	38.8/45.0	39.2/43.9	39.5/51.1	42.4/55.4	38.8/58.2	···	QSS	3C273, PK	···

TABLE II (*continued*)

(1)	(2)	(3)	(4)	(5)	(6)	(7)	(8)	(9)	(10)	(11)	(12)	(13)
				Flux densities								
Source name	Right ascension 1950.0	Declination 1950.0	b	1.4 GHz	2.7 GHz	6.6 GHz	8.0 GHz	10.6 GHz	13.5 GHz	ID	Other names	Note
1330+02	13 30 22.6 ±1.1	+02 16 12 ± 5	+63	3.02±0.12	1.92±0.04	1.14±0.11	1.07±0.02	0.97±0.06	···	GAL	3C287.1, PK	···
1434+03	14 34 25.92±0.07	+03 37 13 ± 1	+55	2.86±0.07	1.83±0.09	1.05±0.14	0.92±0.04	0.71±0.03	···	□	4C+3.30, PK	···
1456+04	14 56 29.6 ±0.2	+04 28 01 ±11	+52	0.93±0.05	0.77±0.04	0.50±0.09	0.59±0.03	···	···	?	4C+4.49	···
1532+01	15 32 20.17±0.02	+01 41 01.7± 0.4	+43	1.18/1.37	1.10±0.04	0.78/1.01	1.08/1.80	1.01/1.28	1.21±0.15	BSO?	PK	A
1535+00	15 35 42.4 ±0.2	+00 28 44 ± 2	+42	0.70±0.04	0.88±0.05	0.72±0.08	0.75±0.04	0.54±0.09	0.65±0.15	?	···	···
1546+02	15 46 58.0 ±0.6	+02 45 50 ±10	+41	0.72±0.09	1.08±0.07	1.75±0.10	1.50/2.34	1.75±0.15	1.27±0.12	QSS	OR078, PK1546+027	···
1555+00	15 55 17.69±0.02	+00 06 43.5± 0.7	+38	1.23/1.89	1.31/2.01	1.85/3.32	1.54/3.14	1.37/3.61	1.26±0.18	BSO	DW, DA393	···
1559+02	15 59 58.5 ±1.8	+02 06 16 ± 3	+38	8.95±0.19	3.77±0.18	1.98±0.07	1.82±0.05	1.52±0.06	···	GAL	3C327, PK	···
1635−03	16 35 39.2 ±0.6	−03 34 17 ±15	+27	0.36±0.04	0.46±0.03	0.40±0.09	0.61±0.03	0.44±0.08	···	GAL	···	···
1648+01	16 48 31.6 ±0.5	+01 34 08 ± 7	+27	0.91±0.05	0.91±0.04	···	0.79/1.15	0.72±0.09	1.07±0.12	□	···	E
1648+05	16 48 40.5 ±0.5	+05 04 32 ± 5	+29	44.4 ±0.7	22.4 ±0.1	···	7.60±0.20	5.24±0.15	···	GAL	3C348, PK, HerA	···
1717−00	17 17 55.6 ±0.5	−00 55 54 ± 4	+20	56.2 ±1.0	34.8 ±0.4	···	15.6 ±0.3	11.5 ±0.3	···	GAL	3C353, PK	···
1741−03	17 41 20.6 ±0.2	−03 48 53 ± 3	+13	1.17/1.86	2.31/2.96	2.39±0.34	3.55±0.15	2.60±0.15	2.22±0.22	Obsc	PK1741−038	···
1949+02	19 49 44.13±0.09	+02 22 42 ± 1	−12	5.85±0.14	3.35±0.11	1.86±0.26	1.68±0.04	1.05±0.06	···	GAL	3C403, PK	···
2044−02	20 44 34.16±0.07	−02 47 27 ± 1	−27	2.24±0.06	1.37±0.04	···	0.92±0.03	0.51±0.02	0.51±0.12	GAL?	3C422, PK, OW−074	···
2059+03	20 59 08.0 ±0.6	+03 30 08 ±30	−27	0.48±0.04	0.68±0.03	···	0.76/1.55	1.04±0.06	0.69±0.10	QSS	OW098, PK2059+034	···
2128+04	21 28 02.62±0.05	+04 49 04.0± 0.6	−32	4.03±0.14	3.04±0.06	1.78±0.12	1.69±0.04	1.36±0.05	···	□	OX046, PK2127+04	···
2131−02	21 31 35.34±0.09	−02 06 40.8± 1.0	−37	1.42/1.80	1.54/1.91	2.06/2.75	1.71/3.39	2.64/3.60	4.17±0.14	BSO?	OX−053, PK2131−021	···
2134+00	21 34 05.22±0.01	+00 28 25.7± 0.4	−36	3.10±0.11	7.20±0.24	12.7 ±0.36	12.4 ±0.11	12.3 ±0.44	···	QSS	OX057, PK2134+004	···
2210+01	22 10 05.17±0.03	+01 37 59.5± 0.4	−42	2.63±0.10	1.68±0.03	···	0.69±0.04	0.55±0.04	0.42±0.15	□	4C1.69, PK, OY016	···
2216−03	22 16 16.3 ±0.1	−03 50 39 ± 2	−47	0.89±0.05	1.00/1.21	1.38/2.02	2.51±0.06	1.43/2.97	2.90±0.36	QSS	4C−3.79, PK, OY−027	B
2254+02	22 54 45.2 ±2.9	+02 27 13 ±16	−49	0.38±0.04	0.36±0.03	···	0.78±0.02	0.72/0.90	0.73±0.12	QSS	OY091.3, PK2254+024	···
2318+04	23 18 12.0 ±0.1	+04 57 25 ± 2	−51	0.98±0.05	1.31±0.03	···	1.48±0.03	1.92±0.15	···	BSO	OZ031	B
2332−01	23 32 46.4 ±0.2	−01 47 48 ± 3	−59	0.62/0.91	0.51±0.02	···	0.39±0.14	···	<0.5	BSO	OZ−055, PK2332−017	···
2335−02	23 35 20.9 ±2.1	−02 47 40 ± 7	−60	0.65±0.04	0.63±0.02	···	0.69±0.08	0.61±0.10	0.63±0.17	BSO	OZ−060, PK2335−027	···

Notes to Table II

A. Position measured at 2.7 and 8.1 GHz with NRAO three-element interferometer (Fomalont, Brandie, and Bridle, unpublished).
B. Confusing source, see Table IV.
C. Extended source, uncertain resolution correction at 8 GHz.
D. See Fomalont (1971) for structure.
E. Part of extended emitting region at 1.4 GHz, see Fig. 1.

TABLE III. Supplementary position and flux-density data used in constructing Table II and the 8-GHz source spectra.

	Positions
365 MHz	Moseley *et al.* 1970; Douglas *et al.* 1973; Ghigo and Owen 1973.
408 MHz	Clarke *et al.* 1969; Munro 1971, 1972; Hunstead 1972; Jauncey and Hunstead 1972.
1.4 GHz	Pauliny-Toth *et al.* 1966; Fomalont 1971; Fomalont and Moffet 1971; Bridle *et al.* 1972a.
2.3 GHz	Cohen and Shaffer 1971.
2.7 GHz	Shimmins *et al.* 1966; Merkelijn 1969; Wills and Bolton 1969; Wade 1970; Wade and Miley 1971; Witzel *et al.* 1971; Adgie *et al.* 1972; Browne *et al.* 1973; Brosche *et al.* 1973.
5.0 GHz	Witzel *et al.* 1971; Pauliny-Toth *et al.* 1972.
7.8 GHz	Cohen 1972.
8.1 GHz	Brosche *et al.* 1973.
	Flux densities
318 MHz	Condon and Jauncey 1974.
408 MHz	Murdoch and Large 1968; Wyllie 1969; Harris 1969; Hunstead 1972; Jauncey and Hunstead 1972.
606 MHz	Condon and Jauncey 1974.
1.4 GHz	Harris 1969; Bridle *et al.* 1972a; Wall 1972; Kellermann *et al.* 1969.
2.7 GHz	Kellermann *et al.* 1968; Wall 1972.
5.0 GHz	Pauliny-Toth and Kellermann 1968; Wall 1972.
6.6 GHz	Kraus and Andrew 1970; Bell *et al.* 1971; Wills *et al.* 1971; Conklin *et al.* 1972; Medd *et al.* 1972.
10.6 GHz	Doherty *et al.* 1969; Kraus and Andrew 1970; Bell *et al.* 1971; Wills *et al.* 1971; Conklin *et al.* 1972; Medd *et al.* 1972; Kellermann and Pauliny-Toth 1973.

for the survey sources and Column (13) refers to notes at the end of the Table.

Table IV lists further sources which were detected within 20 arcmin of the survey sources during the 1.4-GHz mapping observations. These are probably unrelated confusing sources and are listed here merely to document their presence as possible confusing objects for low-resolution observations of the survey sources.

III. OPTICAL IDENTIFICATIONS

Overlays were produced for the *National Geographic Society—Palomar Observatory Sky Survey* using reference star positions from the *Smithsonian Astrophysical Observatory Star Catalog*. The estimated accuracy to which the typical overlay could be positioned on the Sky Survey prints or plates is ~4 arcsec. Although this is considerably less than the accuracy of the most precise positions available for some 8-GHz sources it is usually sufficient to isolate a single candidate for each optical identification. The red and blue Sky Survey prints were inspected at the positions of all 8-GHz sources, regardless of previous documentation of their identifications. Some faint or difficult optical objects were also examined on the plate copy of the Sky Survey at the David Dunlap Observatory.

We have confirmed 40 previously-reported identifications, in many cases using more reliable positions than those available to earlier workers and have obtained new or alternative identifications for 12 other sources (including five empty fields). Table V gives details of the identifications and Plate I (p. 985) gives finding charts for seven objects. An asterisk in column (4) of this Table refers to a note at the end of the table.

The results show a very high rate of identification with stellar objects (56%) compared to the rate of identification with galaxies (27%).

IV. RADIO SPECTRA

A. Numerical Description of the Spectra

The primary data listed in Table II, together with secondary data from the references listed in Table III, were plotted logarithmically against frequency displaying their standard errors. Smooth curves were drawn through the plotted data "by eye," treating the flux-density ranges shown by variable sources as "error bars." We prefer this elementary procedure to formal curve-fitting as it makes no *a priori* assumptions about the analytic forms of the spectra.

Flux densities were interpolated from these curves at four "standard" frequencies (2.0, 3.5, 6.0, and 10.5 GHz) chosen to lie near well-defined data on most of the spectra while defining two spectral "windows" (2.0–3.5 and 6.0–10.5 GHz) of equal harmonic width. The interpolated flux densities were used to derive two spectral indices ($S \propto \nu^{\alpha}$) to characterize the spectral curve of each source—$\alpha_{2.7}$, the index in the "window" centered on 2.7 GHz, and $\alpha_{8.0}$, the index in the 8-GHz window. These indices are listed in Columns (2) and (3) of Table VI.

B. The Radio Two-Color Diagram

Radio spectra are commonly classified according to spectral curvature (e.g., Kellermann *et al.* 1969). The usual (S, C−, C+, Cpx) classification is adequate to describe deviations from basically power-law spectra. Improved flux-density measurements and the availability of high-frequency source surveys have, however, increased the variety of spectral types to be described, making a more refined approach to spectral classification desirable. For example, the C− spectral class contains not only sources with low-frequency turnovers due to self-absorption, but also sources with high-frequency steepening due to E^2-dependent losses. A classification

TABLE IV. Confusing sources.

Survey source	Nearby source	1950.0 R.A.	1950.0 Dec.	1.4-GHz flux density	Separation (arcmin)	P.A. (deg)
0038−02	0038−019	00 38 51.4	−01 59 30	0.86	7.6	63
0055−01	0053−016	00 53 44.8	−01 37 11	2.1	19.3	278
0122−00	0122−003	01 22 38.7	−00 17 31	(0.2)[a]	5.7	314
0122−00	0122−006	01 22 43.6	−00 34 13	0.60	13.0	193
0336−01	0337−021	03 37 45.9	−02 04 07	0.70	14.1	124
0336−01	0335−019	03 36 29.8	−01 42 40	0.47	15.4	332
0442+00	0421+004	04 21 17.1	+00 24 13	1.56	14.8	250
0743−00	0742−007	07 42 47.1	−00 41 53	0.24	9.8	240
0929+04	0829+046	08 29 44.1	+04 33 08	0.23	10.6	130
1148−00	1147−004	11 47 31.7	−00 22 53	0.26	18.4	211
1219+04	1219+048	12 19 20.0	+04 45 31	0.43	17.1	335
2216−03	2215−039	22 15 45.7	−03 56 00	0.13	9.3	235
2318+04	2318+047	23 18 15.6	+04 43 15	0.14	13.8	176

[a] Estimated from $S_{408}=0.56$ Jy (Jauncey and Hunstead 1972) assuming $\alpha=-0.7$.

scheme taking account of spectral curvature without losing spectral-index data would avoid such inadequacies and achieve a more physically realistic separation of source properties.

Figure 2 illustrates a possibly fruitful approach to spectral classification which bears an exact analogy to the $U-B$, $B-V$ plots used by optical astronomers. In this "radio two-color diagram," $\alpha_{2.7}$ is plotted against $\alpha_{8.0}$ for the same source; lines of constant "spectral curvature" $(\alpha_{2.7}-\alpha_{8.0})$ are parallel lines of unit slope. The simplest spectral shapes likely to arise from low-frequency opacity and from E^2-dependent losses are separated in this display even if they have the same "curvature."

The statistics of spectral indices and spectral curvature in a radio source sample can be displayed on such a diagram with minimal loss of information. To assist interpretation of our subsequent discussion, the logarithmic spectral shapes characterized by different areas of the diagram are schematically illustrated in Fig. 2.

A radio two-color diagram for the 8-GHz sources is given in Fig. 3. The reliably-identified galaxies and QSS (closed and open circles, respectively) tend to occupy different regions of the diagram. With the exception of two "deviant" objects (0111+02 and

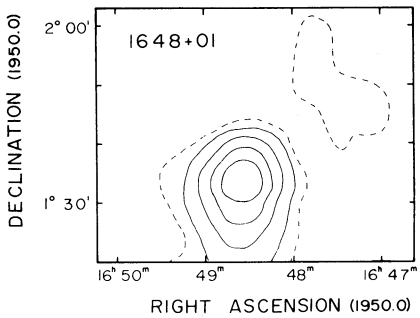

FIG. 1. 1.4-GHz contour map of 1648+01, obtained with the NRAO 300-ft telescope. The contour interval is 0.2 Jy apart from the outer (dotted) contours which are at 0.1 Jy. The half-power beamwidth of the telescope is 9.85 arcmin in right ascension by 10.7 arcmin in declination.

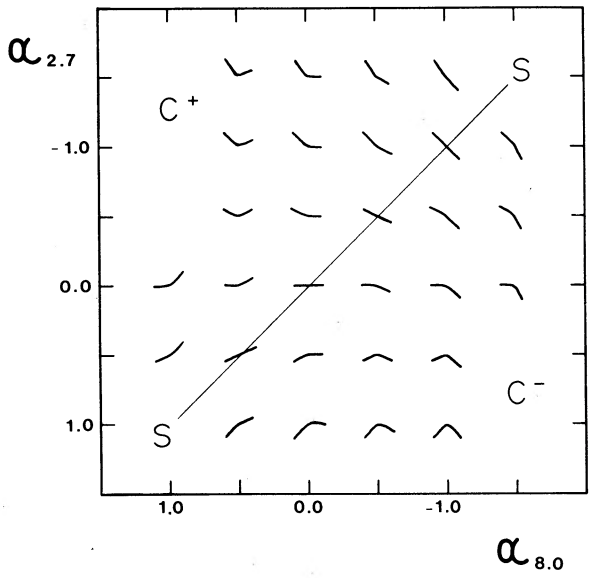

FIG. 2. Radio two-color diagram showing spectral shapes characterized by different regions of the diagram. The unit line is the locus of spectra that would be classified S; spectra lying above the unit line would usually be classified C+ while spectra lying below it would usually be classified C−.

TABLE V. Optical identifications of the Michigan sources.

(1) Source name	(2) Identification	(3) Comment	(4) Note
0034−01	GAL	Confirms Hazard (1965)	
0035−02	GAL	Confirms Wyndham (1966)	
0038−02	QSS	Confirms Bolton and Wall (1970)	
0055−01	GAL	Confirms Wyndham (1966)	
0056−00	QSS	Confirms Bolton *et al.* (1966)	
0106+01	QSS	Confirms Bolton *et al.* (1965)	
0111+02	GAL	Confirms Wall *et al.* (1971); finding chart in Plate I (p. 985)	*
0112−01	BSO	Confirms Bolton and Wall (1970)	
0119+04	BSO	New ID; finding chart in Plate I	
0122−00	QSS	Confirms Bolton *et al.* (1966)	
0123−01	GAL	Confirms Maltby *et al.* (1963)	
0237−02	BSO	Confirms Bolton and Wall (1970)	
0240−00	GAL	Nucleus of NGC 1068	
0305+03	GAL	Confirms Mills (1960)	
0336−01	QSS	Confirms Bolton and Ekers (1966) Finding chart in Kinman *et al.* (1967)	
0404+03	GAL?	See Fomalont (1971)	
0420−01	QSS	Confirms Bolton and Ekers (1966)	
0422−00	?	...	*
0440−00	BSO	Confirms Bolton and Ekers (1966)	
0500+01	□	...	*
0723−00	NSO	Confirms Browne *et al.* (1973)	
0736+01	QSS	Confirms Bolton and Kinman (1966)	
0743−00	NSO	Confirms Bolton and Wall (1970)	
0829+04	NSO	New ID; finding chart in Plate I	
0906+01	QSS	Confirms Bolton, Shimmins, and Merkelijn (1968)	
0922+00	QSS	Confirms Bolton, Kinman, and Wall (1968)	
1055+01	BSO	Confirms Bolton *et al.* (1966)	
1148−00	QSS	Confirms Bolton and Kinman (1966)	
1219+04	BSO	Confirms Bolton *et al.* (1971)	
1226+02	QSS	3C 273	
1330+02	GAL	Confirms Wyndham (1966)	
1434+03	□	...	
1456+04	?	...	*
1532+01	BSO?	Confirms Peterson and Bolton (1973)	*
1535+00	?		*
1546+02	QSS	Confirms Bolton and Wall (1970)	
1555+00	BSO	New ID; finding chart in Plate I	
1559+02	GAL	Confirms Bolton (1960)	
1635−03	GAL	New ID; finding chart in Plate I	
1648+01	□	...	
1648+05	GAL	3C 348, Hercules A	
1717−00	GAL	3C 353	
1741−03	?	...	*
1949+02	GAL	Confirms Wyndham (1966)	
2044−02	GAL?	New ID; finding chart in Plate I	
2059+03	QSS	Confirms Bolton and Wall (1970)	
2128+04	□	...	
2131−02	BSO?	Confirms Bolton and Wall (1970)	*
2134−00	QSS	Confirms Shimmins *et al.* (1968)	
2210+01	□	...	
2216−03	QSS	Confirms Bolton and Ekers (1966)	
2254+02	QSS	Confirms Bolton, Kinman, and Wall (1968)	
2318+04	BSO	Probably confirms Pauliny-Toth *et al.* (1972); finding chart in Plate I	
2332−01	BSO	Confirms Bolton and Wall (1970)	
2335−02	BSO	Confirms Bolton and Wall (1970)	

Symbols used in column (2)

GAL—Galaxy
GAL?—Probably a galaxy.
QSS—Quasi-stellar source with a measured redshift.
BSO—Blue stellar object; redshift not measured.
NSO—Stellar object of neutral color; redshift not measured.
□—Empty field at radio position.
?—Identification unknown; see notes.

Notes to Table V

0111+02. Our position, measured with the NRAO interferometer, coincides with the galaxy marked in the finding chart in Plate I, but there is a radio-quiet BSO 30 arcsec south and 13 arcsec west of the galaxy.

0422+00. Our position, measured with the NRAO interferometer, is very close to the object identified by Bolton, Shimmins, and Merkelijn (1968). Wall, Shimmins, and Merkelijn (1971) have reported that this object has a stellar spectrum. There are no other visible objects within the error limits of our position.

0500+01. On the basis of our position, we agree with the conclusion of Wall *et al.* (1971) and disagree with the identification proposed by Pauliny-Toth *et al.* (1972).

1456+04. Our position agrees with the stellar object identified by Hazard *et al.* (1970). Wills *et al.* (1973) have reported that this object has a stellar spectrum.

1532+01. The object is reported to have an ultraviolet excess (Peterson and Bolton 1973), but appears slightly diffuse on the red Palomar Sky Survey plate.

1535+00. The nearest object to the radio position is neutral and stellar, but an optical position measured by B. and D. Wills (private communication) suggests that it is probably unrelated to the radio source.

1635−03. The object marked is red and appears diffuse on the Sky Survey plates.

1741−03. There are several faint red objects near the radio position, but this is a region of heavy interstellar obscuration.

2044−02. The object marked in Plate I is slightly red and may be slightly diffuse.

2132−02. The object appears slightly elongated on the Sky Survey plates.

1635−03) the galaxies are contained in a conspicuous grouping in the upper right quadrant of the diagram. This grouping forms the basis for a new approach to spectral classification, which we develop in the following section.

C. Spectral Class G

The concentration of the galaxy spectra to a compact region of the diagram suggests that a physically homogeneous spectral class might be characterized by occupancy of a given area of the two-color diagram as first suggested by Bolton (1969). One approach to isolating such a class would be to draw a closed envelope around the actual points in the diagram representing the "nondeviant" galaxy spectra. The size of our sample is so small, however, that such a procedure might under-represent the true range of spectral forms to be associated with such a class. We have therefore defined a "galaxy-like" spectral class by a procedure that takes some account of the small sample size.

Application of Chauvenet's criterion to the separate distributions of $\alpha_{2.7}$ and $\alpha_{8.0}$ for the well-identified galaxies confirmed that the spectra of 0111+02 and 1635−03 are sufficiently deviant to be discarded from the definition of a "standard" galaxy-like population. The spectra of the two "possible galaxy" (GAL?) identifications were examined individually using the same criterion; both sources (0404+03 and 2044−02) have spectra consistent with membership of the "galaxy-like" population. Because some empty-field sources may also be galaxies below the Sky Survey limit, the empty-field spectra were similarly examined. It was found that 1434+03, 2128+04, and 2210+01 have spectra consistent with membership of the "galaxy-like" population.

We therefore define spectral class "G" from the observed properties of the reliably-identified galaxies other than 0111+02 and 1635−03, plus the "possible galaxies" 0404+03 and 2044−02 and the empty fields 1434+03, 2128+04, and 2210+01. The boundary of class G in the two-color diagram was established by using Chauvenet's criterion to trace the elliptical locus of the most deviant spectra that could be added to those of the defining sources without rejection. The nomenclature was chosen to reflect the identification content

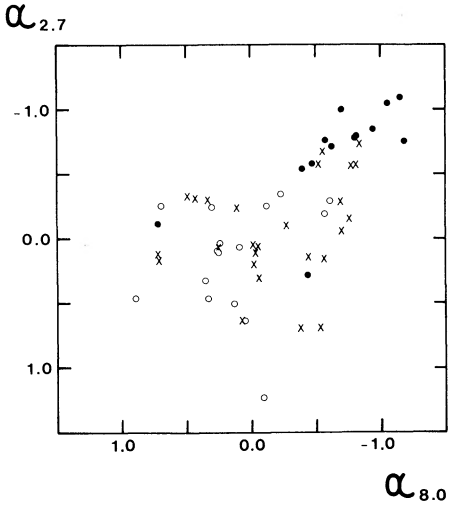

FIG. 3. Radio two-color diagram of the 8-GHz sources. Symbols: ○—quasars, ●—galaxies, ×—less certain identifications.

TABLE VI. Spectral properties of the 8-GHz sources.

(1) Source name	(2) $\alpha_{2.7}$	(3) $\alpha_{8.0}$	(4) V_{max}	(5) Optical identification	(6) Spectral class
0034−01	−0.79	−0.80	0	GAL, z=0.0733	G
0035−02	−0.72	−0.62	?	GAL, z=0.2201	G
0038−02	+0.03	+0.24	?	QSS, z=1.176	Q2
0055−01	−0.77	−0.57	0	GAL, z=0.0450	G
0056−00	−0.35	−0.23	0.06	QSS, z=0.717	GQ
0106+01	+0.63	+0.05	0.46	QSS, z=2.107	Q2
0111+02	−0.12	+0.72	?	GAL	Q3
0112−01	+0.10	−0.03	0.22	BSO	Q1
0119+04	+0.31	−0.06	0	BSO	Q1
0122−00	−0.26	+0.69	0.18	QSS, z=1.070	Q3
0123−01	−1.10	(−1.15)	0	GAL, z=0.018	G
0237−02	+0.63	+0.07	0	BSO	Q2
0240−00	−0.86	−0.94	0	GAL, z=0.00377	G
0305+03	−0.59	−0.47	0	GAL, z=0.289	G
0336−01	+0.10	+0.25	0.41	QSS, z=0.852	Q2
0404+03	−0.68	−0.55	0	GAL?	G
0420−01	+0.06	+0.09	0.37	QSS, z=0.915	Q2
0422+00	−0.24	+0.11	0.51	?	Q3
0440−00	−0.07	−0.70	0.37	BSO	GQ
0500+01	−0.16	−0.76	0	□	GQ
0723−00	−0.11	−0.27	0.24	NSO	GQ
0736+01	−0.20	−0.57	0.31	QSS, z=0.191	GQ
0743−00	+0.69	−0.38	0.27	NSO	Q1
0829+04	+0.06	+0.25	0.37	NSO	Q2
0906+01	−0.25	+0.30	0.33	QSS, z=1.018	Q3
0922+00	−0.26	−0.12	0.45	QSS, z=1.72	GQ
1055+01	+0.05	−0.01	0.26	BSO	Q1
1148−00	−0.30	−0.61	0	QSS, z=1.982	GQ
1219+04	+0.20	−0.02	0.38	BSO	Q1
1226+02	+0.09	+0.26	0.20	QSS, z=0.158	Q2
1330+02	−0.55	−0.39	0	GAL, z=0.2156	G
1434+03	−0.58	−0.81	0	□	G
1456+04	−0.33	+0.49	?	?	Q3
1532+01	−0.32	+0.43	0.25	BSO	Q3
1535+00	+0.15	−0.56	?	?	Q1
1546+02	+0.50	+0.13	0.22	QSS, z=0.412	Q2
1555+00	+0.14	−0.44	0.45	BSO	Q1
1559+02	−1.01	−0.70	0	GAL, z=0.1041	G
1635−03	+0.28	−0.43	?	GAL	Q1
1648+01	−0.30	+0.33	0.19	□	Q3
1648+05	−1.06	−1.05	?	GAL, z=0.154	G
1717−00	−0.81	−0.81	0	GAL, z=0.0307	G
1741−03	+0.68	−0.53	0.23	Obscured	Q1
1949+02	−0.76	−1.18	0	GAL, z=0.0590	G
2044−02	−0.57	−0.77	?	GAL?	G
2059+03	+0.46	+0.33	0.34	QSS, z=0.370	Q2
2128+04	−0.58	−0.52	0	□	G
2131−02	+0.17	+0.71	0.33	BSO?	Q2
2134+00	+1.22	−0.09	0	QSS, z=1.94	Q1
2210+01	−0.74	−0.84	?	□	G
2216−03	+0.46	+0.89	0.35	QSS, z=0.901	Q2
2254+02	+0.32	+0.35	0.11	QSS, z=2.09	Q2
2318+04	+0.12	+0.72	0	BSO	Q2
2332−01	−0.29	−0.69	0.19	BSO	GQ
2335−02	+0.06	−0.05	?	BSO	Q1

of the spectral class. No QSS in the sample has a spectrum within the class G boundary. This boundary therefore separates all the QSS from 85% of the galaxies in the 8-GHz survey.

The two galaxies which do not have class G radio spectra exhibit no striking peculiarities on the Sky Survey prints, except that a very blue stellar object lies only ~30 arcsec from 0111+02 [see Plate I (p.

985)]. Our observations with the NRAO interferometer show that this blue object is definitely not responsible for the observed radio emission.

D. Spectral Classes Q and GQ

The confirmed QSS (i.e., those with measured redshifts) have spectra which are more scattered in the two-color diagram than those of the galaxies. There is no closely-grouped "quasar-like" spectral class comparable to class G. Only one QSS (2134+00) has a radio spectrum significantly deviant from the others in the sample according to Chauvenet's criterion. The unusual feature of this spectrum is $\alpha_{2.7}=+1.22$; the low-frequency turnover of the spectrum is *unusually abrupt*, perhaps implying unusually homogeneous conditions in the source.

Inspection of the two-color diagram shows that 55% of the confirmed QSS (open circles in Fig. 3) lie in the area where both $\alpha_{2.7}$ and $\alpha_{8.0}$ are positive (i.e., the source spectrum peaks at a frequency above 8 GHz). Thus, the most characteristic spectral feature of the QSS is intense high-frequency (~10 GHz) radiation. We have, therefore, divided the two-color diagram outside the class G boundary into four regions, which differ in the degree to which they display this characteristic. Class "Q" comprises three regions in which at least one of $\alpha_{2.7}$ and $\alpha_{8.0}$ is positive. These are

Q1: $\alpha_{2.7}$ positive, but $\alpha_{8.0}$ negative (spectrum peaks below 8 GHz),
Q2: $\alpha_{2.7}$ positive, and $\alpha_{8.0}$ positive (spectrum peaks above 8 GHz),
Q3: $\alpha_{2.7}$ negative, but $\alpha_{8.0}$ positive (spectrum peaks above 8 GHz, but also has a *strong* lower-frequency component).

The remaining region of the two-color diagram, lying outside both the elliptical class G boundary and the L-shaped class Q boundary (see Fig. 4), is given the hybrid designation GQ. Of the sixteen confirmed QSS in the 8-GHz survey, nine have class Q2 spectra, four class GQ, two class Q3, and one class Q1. The QSS with GQ spectra (0056−00, 0736+01, 0922+00, and 1148−00) resemble the "galaxy-like" class G sources in having both $\alpha_{2.7}$ and $\alpha_{8.0}$ negative, but are quasar-like in having a greater proportion of high-frequency emission than the members of that class. The spectral class assigned to each 8-GHz source is listed in Column (6) of Table VI.

E. Stellar Objects, Empty Fields, and Unidentified Sources

Figure 5 shows the radio two-color diagram for the stellar objects without measured red shifts, the empty fields, and the four unidentified sources. The boundaries of the G, GQ, Q1, Q2, and Q3 spectral classes are also shown. The spectra of all the stellar objects are consistent with their being QSS.

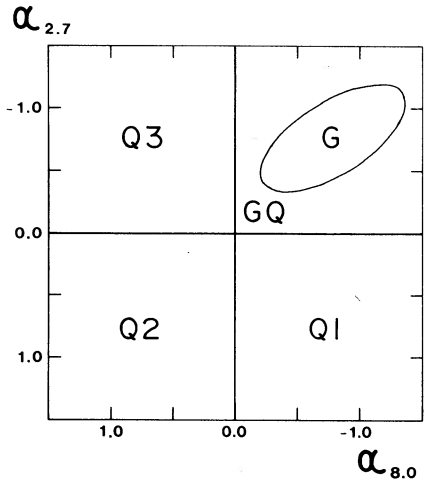

FIG. 4. Radio two-color diagram showing spectral-class boundaries. The elliptical boundary of class G has the following parameters—center: (−0.76, −0.76), semimajor axis: 0.67, semiminor axis: 0.29, inclination to $\alpha_{8.0}$ axis: 32°.5.

The empty fields 0500+01 and 1648+01 have spectra of class GQ and Q3, respectively. Thus, neither is very likely to be a galaxy. The three remaining empty fields form part of the sample used to define spectral class G (see Sec. IV-C).

The four unidentified sources have spectra of classes Q1 and Q3 and are therefore unlikely to be galaxies.

F. Correlation with Red Shifts

Figure 6 shows the distribution of measured redshifts in the two-color diagram. In order to examine whether the emitted spectral forms vary systematically with redshift, the spectral indices used to plot Fig. 6 were

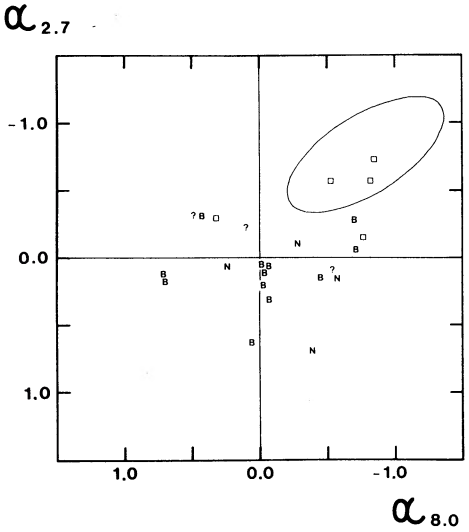

FIG. 5. Radio two-color diagram of sources identified as blue stellar objects, neutral stellar objects, empty fields, or unknown identification. The boundaries of the different spectral regions are shown. Symbols: B—Blue stellar object, N—neutral stellar object, □—empty field, ?—unknown identification.

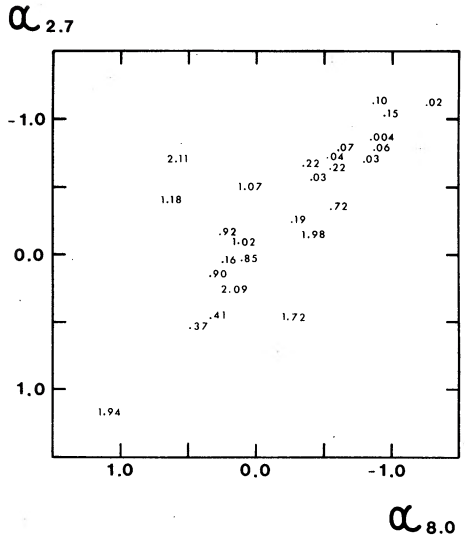

FIG. 6. K-corrected radio two-color diagram for sources with measured redshifts.

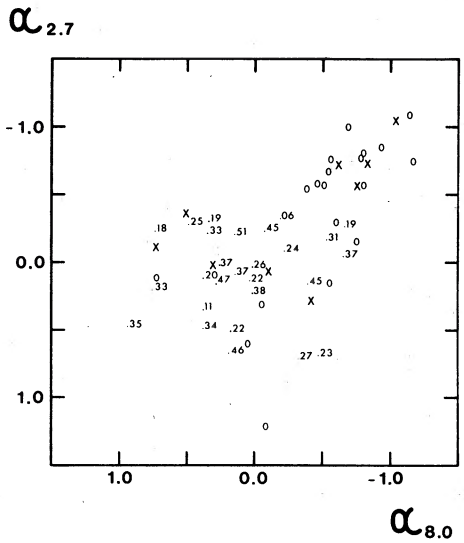

FIG. 8. Radio two-color diagram for sources classified according to variability index V (see text).

determined at 2.7 and 8.0 GHz in the rest-frames of the emitters. There is no general correlation between the redshift and spectral class other than the galaxy-QSS separation already discussed. In particular, there is no correlation between redshift and location in the two-color diagram within class Q.

V. VARIABILITY

Figure 7 shows the two-color diagram for all sources in the 8-GHz survey classified according to whether or not they are known to vary at any frequency. The sources have not been equally extensively monitored, but some significant trends may, nevertheless, be noted.

Firstly, sources with class G spectra are rarely variable, if at all. Fully 75% of the sources with class G spectra have been well-monitored and found not to vary significantly, while none is definitely variable. In contrast, 70% of the sources with non-G spectra (including class GQ) are definitely variable.

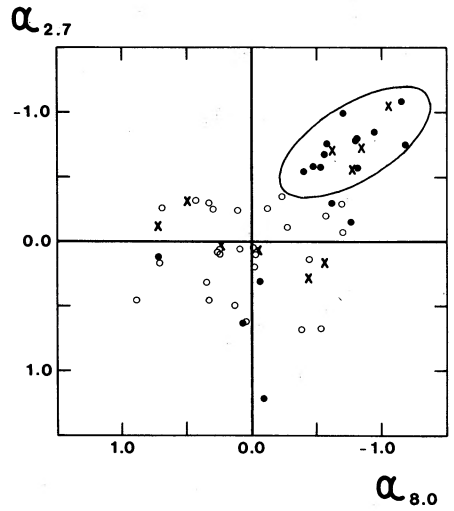

FIG. 7. Radio two-color diagram for sources classified according to observed variability. Symbols: o—variable, ●—not significantly variable, ×—insufficiently monitored.

Secondly, only two of sixteen confirmed QSS are *not* observed to vary significantly. These two (1148−00 and 2134+00) both have spectra on the outer fringe of the two-color plot for QSS and have very similar redshifts (1.982 and 1.94, respectively). They are not spectrally similar however: 1148−00 has the steepest high-frequency spectrum among the survey QSS ($\alpha_{8.0}=-0.61$) while 2134+00 has the most abrupt cutoff below ~6 GHz ($\alpha_{2.7}=+1.22$).

Sixty per cent of the class Q1 sources (6 of 10) are variable, as are 67% of class Q2 (8 of 12), and 70% of class GQ (5 of 7), compared with 80% of class Q3 (8 of 10). These statistics suggest that the class GQ spectra are more closely related to class Q than to class G. There is a trend, significant only at the 83% level, for variability to be more common going from class Q1 to class Q3 in the two-color diagram. This possible trend should be investigated in larger samples.

The degree of varability of a source at any frequency can be described by a variability "index"

$$V=\frac{S_{\max}-S_{\min}}{S_{\max}+S_{\min}},$$

where $S_{\max}$ and $S_{\min}$ are the maximum and minimum flux densities observed at that frequency. Column (4) of Table VI gives the maximum value of V found at any frequency for each source. A question mark in this column indicates that the source has not been monitored often enough for lack of variation to be considered significant. Figure 8 is a two-color diagram indicating these values of V. There is no clear correlation between the maximum V and the spectral class of a source,

except for the general separation between classes G and non-G described above. We also found no correlation between spectral class and the time-scale for significant variations.

VI. COMPARISON WITH SURVEYS AT OTHER FREQUENCIES

The Michigan 8-GHz survey has provided a sample of sources for which a very high rate of optical identification is possible. Of the 50 sources in the survey at $|b|>20°$ only eight have not been identified either as galaxies or as stellar objects. Two of these (0422+00 and 1456+04) lie close to objects reported to be stars, and five are empty fields. The identification rate in low-frequency surveys reaching comparable numbers of sources per steradian has been much lower; for example, almost 30% of the sources with $|b|>20°$ in the *Revised 3C Catalogue* (Bennett 1962) remain unidentified. The rate of identification with stellar objects (56% of all sources) is also much higher than that in lower-frequency surveys; only 18% of high-latitude *Revised 3C* sources are identified with stellar objects.

It has been hypothesized (e.g., Harris 1970) that the low-frequency empty fields are powerful radio galaxies so distant that their optical images are too faint to register on the Palomar Sky Survey plates. The present sample, although small, demonstrates that not all

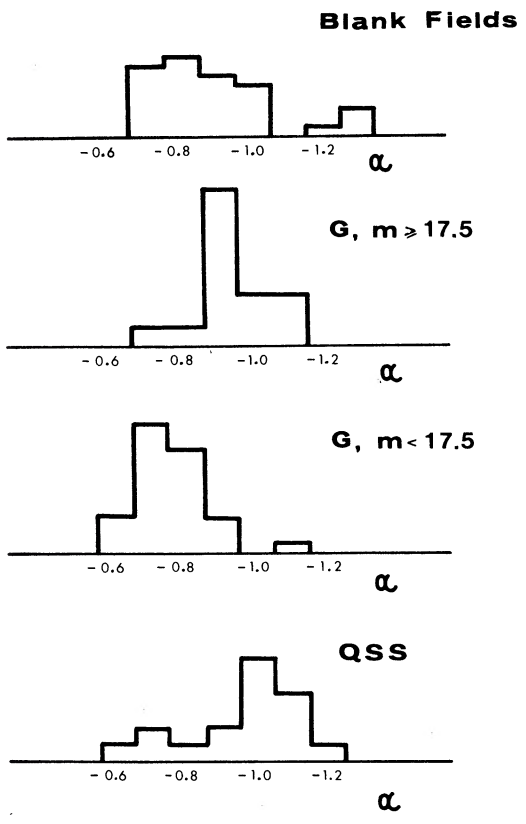

FIG. 9. Distributions of power-law spectral indices for empty fields, galaxies brighter than $m_{pg}=17.5$, galaxies fainter than $m_{pg}=17.5$, and quasars selected at low frequencies (after Roger *et al.* 1973).

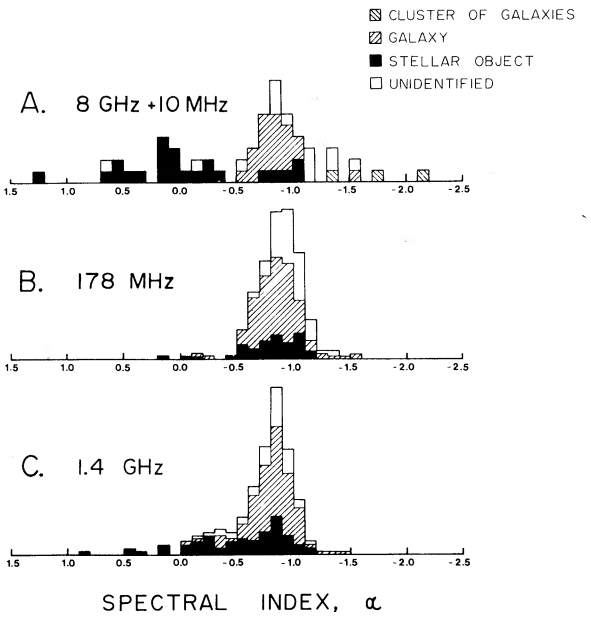

FIG. 10. Distributions of spectral indices near 2 GHz for three source samples. (A) The thirty brightest sources from the present 8-GHz survey and the thirty brightest from the 10-MHz survey of Bridle and Purton (1968). (B) Sources with $|b|>10°$ from the 178-GHz Revised 3C Catalog (after Kellermann *et al.* 1969). (C) Sources with $|b|>20°$ from the 1.4-GHz catalog of Bridle, Davis, Fomalont, and Lequeux (1972a).

empty fields are likely to be of this kind. As was shown in Fig. 5, the empty fields in the 8-GHz survey have radio spectra of both class Q and class G. Those with non-G spectra are unlikely to be galaxies. The class G empty field sources do not have especially steep high-frequency spectra, as might be expected from the spectrum-luminosity relation (Bridle, Kesteven, and Guindon 1972b) if all such objects were extremely distant galaxies. Thus, at 8 GHz, the empty fields are probably a mixed population of QSS and galaxies, the lack of optical counterparts being due as much to low optical luminosity as to great distance of the sources.

Conspicuously absent from the 8-GHz survey are the QSS with class G spectra found at lower frequencies. Figure 9, using data from Roger *et al.* (1973), shows that among class G sources found in low-frequency surveys, the QSS have *steeper* high-frequency power-law spectra than do the galaxies. Thus, it is to be expected that the 8-GHz survey should discriminate more against G-type QSS than against G-type galaxies.

The known range of spectral indices of extragalactic sources is illustrated in the synthetic distribution given in Fig. 10(a), which shows the spectral indices near 2 GHz for the thirty strongest sources in the Michigan 8-GHz survey, and the thirty strongest sources in the Penticton 10-MHz survey (Bridle and Purton 1968). The range of spectral indices of the QSS (+1.22 to −1.01) is more than twice that of the galaxies (−0.66 to −1.56). The median index of the QSS is +0.09, while that of the galaxies is −0.81.

Radio source surveys systematically discriminate in favor of sources whose spectra have a high proportion of their flux density near the survey frequency. Figures 10(b) and 10(c) show spectral-index distributions for sources selected at 178 MHz (Kellermann *et al.* 1969) and 1.4 GHz (Bridle, Davis, Fomalont, and Lequeux 1972a), intermediate between the extremes combined in Fig. 10(a). Comparison of Fig. 10(b) with Fig. 10(a) illustrates that the 178-MHz sample preferentially selects sources, both galaxies and QSS, with class G spectra while discriminating severely against the very steep spectra of extended ($\sim$1 Mpc) sources in clusters of galaxies and against the spectra of our class Q. This selectivity leads to the familiar very strong peak in the index distribution near -0.75. The 1.4-GHz sample [Fig. 10(c)] similarly selects against the cluster sources, but contains examples of the full range of class Q spectra. It still suggests, however, that the most common index in the class Q population is as negative as -0.3. The present 8-GHz survey discriminates seriously against the extended cluster sources and the steeper spectra of class G, especially those of G-type QSS, while favoring those of compact ($\ll$100 kpc) Q-type QSS.

None of the survey samples, of course, represents a source population characteristic of a typical volume of space. The purpose of these comparisons is to emphasize the inadequacies of present surveys at *any* one frequency in obtaining representative samples of extragalactic sources for theoretical studies.

VII. CONCLUSIONS

We have obtained positions, optical identifications, and microwave spectra for 55 sources found in an unbiased survey of $\sim$0.8 steradians of sky at 8 GHz. The principal results are

(1) Over 83% of the survey sources have optical counterparts on the Palomar Sky Survey, more than two-thirds of these being stellar objects whose radio spectra and variability suggest that they are quasars. Some of these objects are neutral in color and may be quasars of very high redshift similar to OH471 (Carswell and Strittmatter 1973) and OQ172 (Wampler *et al.* 1973).

(2) A radio equivalent of the optical "two-color diagram" is valuable when displaying and classifying radio spectral data. Some shortcomings of the common (S, C$-$, C+, Cpx) classification may be overcome by the use of this diagram (Sec. IV-B). The spectral windows used in this paper were chosen for convenience alone and other choices may be more fundamental or revealing.

(3) The radio two-color diagram for the 8-GHz survey sources suggests a division of spectral types into two main classes which we have denoted G and Q to reflect their main identification content—100% galaxies plus empty fields, and 80% probable quasars, respectively.

(4) Class G (30% of the survey sources) is composed entirely of nonvariable radio galaxies and empty fields. The spectra of these empty fields do not suggest that they are galaxies of higher-than-average radio luminosity. Class G corresponds to the main *spectral* population in low-frequency samples such as the *Revised 3C Catalogue*. It should be noted that class G does not consist solely of sources with S-type spectra on the usual classification. Indeed, if classifying a larger high-frequency sample than ours, class G might usefully be subdivided into GS, G$-$, and G+ classes to reflect the original intention of the (S, C$-$, C+) scheme.

(5) Class Q (55% of the survey sources) contains radio-variable stellar objects with only a small (6%) proportion of "deviant" galaxies. This spectral class is much less concentrated in the two-color diagram than is class G. A tentative division into three subclasses has been proposed, reflecting different proportions of emission in spectral windows centered on 2.7 and 8.0 GHz. Over half of the confirmed quasars fall into the class Q2 which has the highest proportion of the observed flux density in the 8-GHz window.

(6) The "hybrid" spectral class GQ (15% of the survey sources) is composed mainly of radio-variable stellar objects and therefore bears stronger affinity to class Q than to class G.

(7) Within class Q there is little correlation between spectral type and redshift or between spectral type and variability.

(8) The two quasars with redshifts closest to the "1.95 peak" have different but unusual radio spectra and are the only confirmed quasars in the sample to show no significant time variations.

(9) Combination of spectral data on sources from this survey with that on sources from a 10-MHz survey [Fig. 10(a)] emphasizes that surveys at extreme radio frequencies reveal sources whose properties differ greatly from those with class G spectra. Extreme source types are the compact QSS with opaque spectra of class Q2 and the Mpc-scale steep-spectrum emission from clusters of galaxies. No single radio survey presently provides a fully representative sample of extragalactic sources.

ACKNOWLEDGMENTS

We thank the Director of the National Radio Astronomy Observatory and the Programming Committee of the Algonquin Radio Observatory for allocating observing time for this investigation. We also thank Dr. H. D. Aller, Dr. E. B. Fomalont, Dr. F. T.

Haddock, and Dr. M. J. L. Kesteven for advice and assistance, and the technical staff of the Michigan 85-ft, NRAO 300-ft, and ARO 150-ft telescopes for their part in the observations. This research was supported by an NSF Grant at the University of Michigan and by grants from the National Research Council of Canada and the Advisory Research Committee at Queen's University.

REFERENCES

Adgie, R. L., Crowther, J. H., and Gent, H. (1972). Mon. Not. Roy. Astron. Soc. **159**, 233.
Bell, M. B., Seaquist, E. R., and Braun, L. D. (1971). Astron. J. **76**, 524.
Bennett, A. S. (1962). Mem. Roy. Astron. Soc. **68**, 563.
Bolton, J. G. (1960). Obs. Owens Valley Radio Observatory No. 5.
Bolton, J. G. (1969). Astron. J. **74**, 131.
Bolton, J. G., and Ekers, J. (1966). Aust. J. Phys. **19**, 559.
Bolton, J. G., and Kinman, T. D. (1966). Astrophys. J. **145**, 951.
Bolton, J. G., and Wall, J. V. (1970). Aust. J. Phys. **23**, 789.
Bolton, J. G., Clarke, M. E., Sandage, A., and Véron, P. (1965). Astrophys. J. **142**, 1289.
Bolton, J. G., Kinman, T. D., and Wall, J. V. (1968). Astrophys. J. **154**, L105.
Bolton, J. G., Shimmins, A. J., and Merkelijn, J. (1968). Aust. J. Phys. **21**, 81.
Bolton, J. G., Shimmins, A. J., Ekers, J., Kinman, T. D., Lamla, E., and Wirtanen, C. A. (1966). Astrophys. J. **144**, 1229.
Bolton, J. G., Wall, J. V., and Shimmins, A. J. (1971). Aust. J. Phys. **24**, 889.
Brandie, G. W. (1972a). Ph.D. Thesis, University of Michigan.
Brandie, G. W. (1972b). Astron. J. **77**, 197.
Bridle, A. H., and Purton, C. R. (1968). Astron. J. **73**, 717.
Bridle, A. H., Davis, M. M., Fomalont, E. B., and Lequeux, J. (1972a). Astron. J. **77**, 405.
Bridle, A. H., Kesteven, M. J. L., and Guindon, B. (1972b). Astrophys. Lett. **11**, 27.
Brosche, P., Wade, C. M., and Hjellming, R. M. (1973). Astrophys. J. **183**, 805.
Browne, I. W. A., Crowther, J. H., and Adgie, R. L. (1973). Nature **244**, 146.
Carswell, R. F., and Strittmatter, P. A. (1973). Nature **242**, 294.
Clarke, T. W., Frater, R. H., Large, M. I., Munro, R. E. B., and Murdoch, H. S. (1969). Aust. J. Phys. Astrophys. Suppl. No. 10.
Cohen, M. H. (1972). Astrophys. Letts. **12**, 81.
Cohen, M. H., and Shaffer, D. B. (1971). Astron. J. **76**, 91.
Condon, J. J., and Jauncey, D. L. (1974). Astron. J. **79**, 437.
Conklin, E. K., Andrew, B. H., Wills, B. J., and Kraus, J. D. (1972). Astrophys. J. **177**, 303.
Davis, M. M. (1971). Astron. J. **76**, 980.
Dent, W. A. (1965). Science **148**, 1458.
Dent, W. A. (1972). Astrophys. J. **177**, 93.
Dent, W. A., and Haddock, F. T. (1965). Nature **205**, 487.
Dent, W. A., and Haddock, F. T. (1966). Astrophys. J. **144**, 568.
Doherty, L. H., MacLeod, J. M., and Purton, C. R. (1969). Astron. J. **74**, 827.
Douglas, J. N., Bash, F. N., Ghigo, F. D., Moseley, G. F., and Torrence, G. W. (1973). Astron. J. **78**, 1.
Ekers, J. A. (ed.) (1969). Aust. J. Phys. Astrophys. Suppl. No. 7.
Fomalont, E. B. (1971). Astron. J. **76**, 513.
Fomalont, E. B., and Moffet, A. T. (1971). Astron. J. **76**, 5.
Ghigo, F. D., and Owen, F. N. (1973). Astron. J. **78**, 848.
Harris, B. J. (1969). Ph.D. Thesis, Australian National University.
Harris, B. J. (1970). In *External Galaxies and Quasi-stellar Objects*, edited by D. S. Evans, I.A.U. Symposium No. 44, p. 232.
Hazard, C. (1965). In *Quasi-stellar Sources and Gravitational Collapse*, edited by I. Robonson, A. Schild, and E. L. Schucking, First Texas Symposium on Relativistic Astrophysics, p. 135.
Hazard, C., Jauncey, D. L., and Backer, D. C. (5970). Astron. J. **75**, 1039.
Hunstead, R. W. (1972). Mon. Not. Roy. Astron. Soc. **157**, 367.
Jauncey, D. L., and Hunstead, R. W. (1972). Astron. J. **77**, 345.
Katgert, P., Katgert-Merkelijn, J. K., Le Poole, R. S., and Laan, H. van der (1973). Astron. Astrophys. **23**, 171.
Kellermann, K. I., and Pauliny-Toth, I. I. K. (1973). Astron. J. **78**, 828.
Kellermann, K. I., Pauliny-Toth, I. I. K., and Tyler, W. C. (1968). Astron. J. **73**, 298.
Kellermann, K. I., Pauliny-Toth, I. I. K., and Williams, P. J. S. (1969). Astrophys. J. **157**, 1.
Kinman, T. D., Bolton, J. G., Clarke, R. W., and Sandage, A. (1967). Astrophys. J. **147**, 848.
Kraus, J. D., and Andrew, B. H. (1970). Astrophys. J. **159**, L41.
Maltby, P., Matthews, T. A., and Moffet, A. T. (1963). Astrophys. J. **137**, 153.
Medd, W. J., Andrew, B. H., Harvey, G. A., and Locke, J. L. (1972). Mem. Roy. Astron. Soc. **77**, 109.
Merkelijn, J. K. (1969). Aust. J. Phys. **22**, 237.
Mills, B. Y. (1960). Aust. J. Phys. **13**, 550.
Moseley, G. F., Brooks, C. C., and Douglas, J. N. (1970). Astron. J. **75**, 1015.
Munro, R. E. B. (1971). Aust. J. Phys. **24**, 617.
Munro, R. E. B. (1972). Aust. J. Phys. Astrophys. Suppl. No. 22.
Murdoch, H. S., and Large, M. I. (1968). Mon. Not. Roy. Astron. Soc. **141**, 377.
Pauliny-Toth, I. I. K., and Kellermann, K. I. (1968). Astron. J. **73**, 953.
Pauliny-Toth, I. I. K., and Kellermann, K. I. (1972). Astron. J. **77**, 797.
Pauliny-Toth, I. I. K., Kellermann, K. I., and Davis, M. M. (1970). In *External Galaxies and Quasi-stellar Objects*, edited by D. S. Evans, I.A.U. Symposium No. 44, p. 444.
Pauliny-Toth, I. I. K., Kellermann, K. I., Davis, M. M., Fomalont, E. B., and Shaffer, D. B. (1972). Astron. J. **77**, 265.
Pauliny-Toth, I. I. K., Wade, C. M., and Heeschen, D. S. (1966). Astrophys. J. Suppl. **13**, 65.
Peterson, P. A., and Bolton, J. G. (1973). Astrophys. Letts. **13**, 187.
Roger, R. S., Bridle, A. H., and Costain, C. H. (1973). Astron. J. **78**, 1030.
Shimmins, A. J. (1971). Aust. J. Phys. Astrophys. Suppl. No. 21.
Shimmins, A. J., and Bolton, J. G. (1972). Aust. J. Phys. Astrophys. Suppl. No. 26.
Shimmins, A. J., Clarke, M. E., and Ekers, R. D. (1966). Aust. J. Phys. **19**, 649.
Shimmins, A. J., Searle, L., Andrew, B. H., and Brandie, G. W. (1968). Astrophys. Letts. **1**, 167.
Stull, M. A. (1971). Astron. J. **76**, 1.
Wade, C. M. (1970). Astrophys. J. **162**, 381.
Wade, C. M., and Miley, G. K. (1971). Astron. J. **76**, 101.
Wade, C. M., Gent, H., Adgie, R. L., and Crowther, J. H. (1970). Nature **228**, 146.
Wall, J. V. (1972). Aust. J. Phys. Astrophys. Suppl. No. 24.
Wall, J. V., Shimmins, A. J., and Merkelijn, J. K. (1971). Aust. J. Phys. Astrophys. Suppl. No. 19.
Wampler, E. J., Robinson, L. B., Baldwin, J. A., and Burbidge, E. M. (1973). Nature **243**, 336.
Wills, B. J., Kraus, J. D., and Andrew, B. H. (1971). Astrophys. J. **169**, L87.
Wills, B. J., Wills, D., and Douglas, J. N. (1973). Astron. J. **78**, 521.
Wills, D., and Bolton, J. G. (1969). Aust. J. Phys. **22**, 775.
Wilson, R. W., and Penzias, A. A. (1966). Astrophys. J. **146**, 286.
Witzel, A., Véron, P., and Véron, M. P. (1971). Astron. Astrophys. **11**, 171.
Wyllie, D. V. (1969). Proc. Astr. Soc. Aust. **1**, 234.
Wyndham, J. D. (1966). Astrophys. J. **144**, 459.

1974AJ.....79..903B

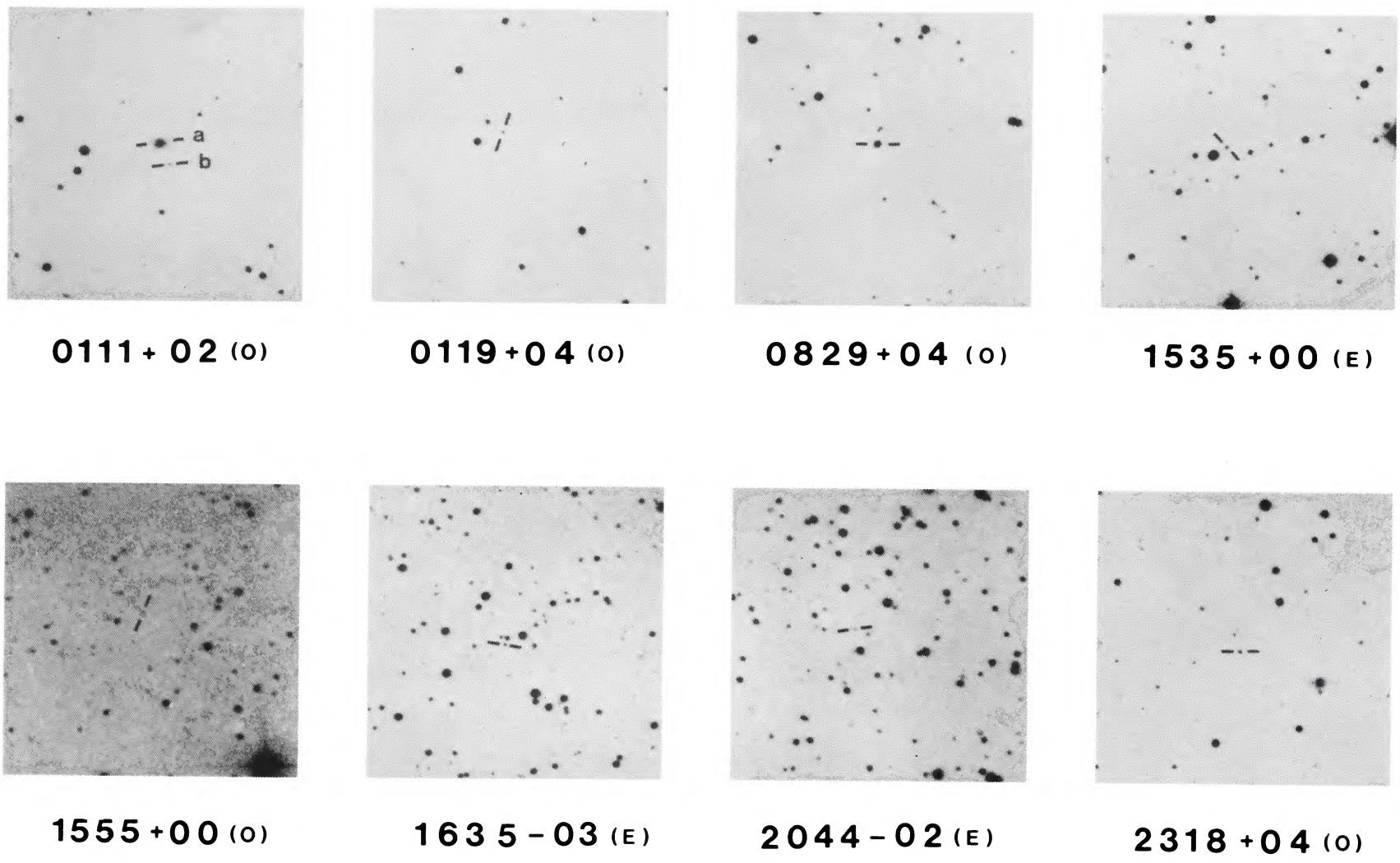

PLATE I (Brandie and Bridle, p. 903). Finding charts for seven sources. Photographs are squares of side 6.8 arcmin. The letter in parenthesis after each source name indicates the Sky Survey print from which the finding chart was made. *0111+02*: The identification is the galaxy (a). Object (b) is blue, stellar (see Sec. IV C). © Copyright National Geographic Society—Palomar Observatory Sky Survey, reproduced courtesy Hale Observatories.